Magnon specific heat and magnetic susceptibility of Fe/Gasb diluted magnetic semiconductor in the presence of applied electric field, magnetic field, and anisotropic energy

Mesefin Birile Woldetsadik, Chernet Amente[*], and P Singh

Department of Physics, Addis Ababa University, PO Box 1176, Addis Ababa, Ethiopia. E-mail: chernet.amente@aau.edu.et

ABSTRACT: Ferromagnetism has been established in a *Fe*-doped ferromagnetic semiconductor *Fe/GaSb* with the Curie-Weiss temperature of 340 *K* for dopant concentration, *x* = 25%. These ferromagnetic semiconductors are very promising candidates for future spintronic devices as they show both semiconducting and magnetic properties. Ferromagnetism can be tuned and controlled by application of electric and magnetic fields, and by radiation. In the present work, the importance of dopant concentration x, effects of electric and magnetic fields, and magnetic anisotropy on the magnon specific heat and magnetic susceptibility of *Fe/GaSb* are studied. Heisenberg localized spin model Hamiltonian with account of nearest neighbor interaction and with the electric and magnetic fields applied, and magnetic anisotropy energy included is second quantized using Holstien-Primakoff transformation to obtain the magnon dispersion from which magnon specific heat and magnetic susceptibility are calculated. Our results show that the magnon specific heat decreases with the increase of magnetic impurity concentration x, while magnetic susceptibility increases. It is also shown that electric and magnetic fields, and magnetic anisotropy can control the magnetic properties of the diluted magnetic semiconductors which are of vital importance for spintronics applications. The results obtained are in broad agreement with experimental and theoretical predictions.

Key words/phrases: Electric field, Magnetic anisotropic energy, Magnetic field, Magnetic susceptibility, Specific heat capacity

INTRODUCTION

A class of materials known as dilute magnetic semiconductors (DMSs) have been a front line research topic since early 1960s (Mauger and Godart, 1986). The pioneering work on the identification of Europium chalcogenides, especially EuO (Matthias *et al.*, 1961), as to posses integrated magnetic and semiconducting properties has motivated the scientific community for the investigation of alternatives presuming doping a small fraction of transition elements into semiconductor crystals circumvent the difficulty of controlling magnetic spin concentration (Furdyna, 1988; Munekata *et al.*, 1989; Ohno *et al.*, 2002; Peaton *et al.*, 2003).

The underlying principle behind ferromagnetism in these materials was the interaction (Yosida, 1957; Dietl *et al.*, 2000) between the itinerant electrons/holes in the semiconductor and the atomic magnetic moments of the dopants via an exchange mechanism which resulted in spin-polarization of carriers in the semiconductor (Furdyna, 1988; Munekata *et al.*, 1989) for the ferromagnetic intervention.

The work by Ohno and Munekata (Munekata *et al.*, 1989; Ohno *et al.*, 2002) on Mn doped InAs aroused curiosity about the possible significance of III-V semiconductors as potential hosts for DMS applications. This field has been advancing rapidly ever since. However, the search for better materials and an understanding of the physical mechanisms underlying the magnetism is an ongoing process.

Control of magnetic phase in DMS is one of the most important processes for magnetic recording and information storage. The use of electric field-controlled magnetization reduces power consumption for storage devices (Ohno *et al.*, 2000; Climente *et al.*, 2005). Electric field control of ferromagnetism was so far demonstrated in a field effect transistor (FET) structure which have been used for non-volatile spin logic devices via carrier-mediated effect (Boukari *et al.*, 2002; Xiu *et al.*, 2010).

Currently there has been tremendous upthrust in research activities on GaSb-based systems (Tu *et*

---
[*]Author to whom correspondence should be addressed.

al., 2015; Tu *et al.*, 2016) especially (Ga,Fe)Sb (Tu *et al.*, 2016). This compound has proved to be an interesting material for both basic and applied research for applications in spintronics (Wolf *et al.*, 2001; Dietl, 2001), which employ the spin degree of freedom of electrons in addition to their charge (Zutic *et al.*, 2004).

Theoretical and experimental analysis show that the specific heat of magnons depend on temperature with the characteristic $T^{1/5}$ (Kane, 2007). However, recent researches demonstrated that the $T^{1/5}$ dependence is not the only attribute as far as the variation may come due to impurity concentration (Twardowski *et al.*, 1991; Bouzerar *et al.*, 2003; Lashkarev *et al.*, 2009) and other defects, such as interstitials, dislocations, voids, etc. The other feature is the ferromagnetic susceptibility dependence since DMS materials are quite temperature sensitive and cease to become ferromagnetic above a temperature known as the Curie temperature T_C, leading merely to paramagnetic (Twardowski *et al.*, 1991; Kane, 2007; Esmailian *et al.*, 2012) and below which spin-glass nature is formed sometimes (Manyala *et al.*, 2008). It is also understood that magnetic impurity interstitials, elements from the group V anti-sites (Sanvito and Hill, 2002) and magneto-crystalline anisotropy are some of factors affecting properties of magnetic impurity doped (III,V) semiconductors. The origin of the anisotropy energy is attributed to be the spin-orbit coupling in the valence band (Jungwith *et al.*, 2006).

In this article, the specific heat capacity and magnetic susceptibility of *Fe/GaSb* DMS system is theoretically studied using a standard model Hamiltonian to explain the response of the material to applied electric and magnetic fields, and magnetic anisotropy energy.

MATERIALS AND METHOD

The model Hamiltonian

The model Hamiltonian constitutes the Heisenberg exchange energy (Hilbert and Nolting, 2005; Jungwith *et al.*, 2006) $\sum_{i,j} J_{ij} \vec{S}_i \cdot \vec{S}_j$ for the designations of spin-spin interaction of the localized spins in Fe^{+3} distributed over sites i and j with exchange energy J_{ij}; the Zeemann energy $-g\mu_B \vec{B} \sum_i S_i^z$ that arises when magnetic field (MF) $\vec{B}$ is applied, where g is the degeneracy factor (or gyromagnetic ratio) and μ_B the Bohr magneton; $-\mu_e \vec{E} \sum_j S_j^z$ due to the interaction of localized moments with the applied electric field (EF), $\vec{E}$; and $\varphi \sum_i (S_i^z)^2$, due to the interaction of localized spins with magnetic anisotropic energy (MAE), φ, where μ_e is the electric dipole moment. Hence,

$$\hat{H} = -\sum_{i,j} J_{i,j} \vec{S}_i \cdot \vec{S}_j - g\mu_B \vec{B} \sum_i \vec{S}_i^z - \mu_e \vec{E} \sum_j \vec{S}_j^z + \varphi \sum_j \vec{S}_i^z \qquad (1)$$

For i and j spin sites $\vec{S}_i \cdot \vec{S}_j = \frac{1}{2}[(S_i^+ S_j^-) + (S_i^- S_j^+)] + S_i^z S_j^z$, where $S^\pm = S_x \pm iS_y$.

The atomic spin operators can be converted into a more standard many-body interaction problem by replacing the spins with boson creation and annihilation operators $\hat{a}_i$ and $\hat{a}_i^+$, respectively, using the Holstein-Primakoff (HP) transformation (Holstein and Primakoff, 1940), $S_i^+ = [2xS(1 - \frac{\hat{a}_i^+ \hat{a}_i}{2xS})]^{1/2} \hat{a}_i$; $S_i^- = \hat{a}_i^+ [2xS(1 - \frac{\hat{a}_i^+ \hat{a}_i}{2xS})]^{1/2}$ and $S_i^z = xS - \hat{a}_i^+ \hat{a}_i$; where S and x are, respectively, total magnetic spin

per atom and concentration of magnetic ions at the cation sites (Chernet Amente, 2018).

Restricted to the lowest powers and hence, ignoring spin wave scattering, $S_i^+ = \sqrt{2xS}\hat{a}_i$; $S_i^- = \sqrt{2xS}\hat{a}_i^+$, an approximation around the state of saturation magnetization, and $S_i^z = xS - \hat{n}_i$, where $\hat{n}_i = \hat{a}_i^+ \hat{a}_i$ represents spin reversal.

Using the aforementioned terminologies and making rearrangements the system Hamiltonian can be written in the form of:

$$\hat{H} = -J\sum_{i,\delta}[xS(\hat{a}_i\hat{a}_{i+\delta}^+ + \hat{a}_i^+\hat{a}_{i+\delta}) + x^2S^2 - xS(\hat{a}_{i+\delta}^+\hat{a}_{i+\delta} + \hat{a}_i\hat{a}_i^+) + \hat{a}_i^+\hat{a}_i\hat{a}_{i+\delta}^+\hat{a}_{i+\delta}]$$

$$-2\mu_B\vec{B}\sum_i(xS - \hat{a}_i^+\hat{a}_i) - \mu_e\vec{E}\sum_{i,\delta}(xS - \hat{a}_{i+\delta}^+\hat{a}_{i+\delta}) + \varphi\sum_i(xS - \hat{a}_i^+\hat{a}_i)^2 \tag{2}$$

Here an average of $J_{ij} = J$ is considered and δ represents the nearest-neighbor distance.

Propagations of spin deviations are described by the Fourier transformations, $\hat{a}_i = \frac{1}{\sqrt{N}}\sum_k\hat{a}_ke^{i\vec{k}\cdot\vec{r}_i}$ and $\hat{a}_i^+ = \frac{1}{\sqrt{N}}\sum_k\hat{a}_k^+e^{-i\vec{k}\cdot\vec{r}_i}$, where $\vec{r}_i$ is the vector from an arbitrary origin to the ith atom, whose magnitude measures the corresponding distance in units of the lattice constant (Holstein and Primakoff, 1940). The Fourier variables, $\hat{a}_k$ and $\hat{a}_k^+$ also satisfy the bosonic relations $[\hat{a}_k, \hat{a}_{k'}^+] = \delta_{k,k'}$, hence, Eq. (1) would be simplified to

$$\hat{H} = -2JxS\sum_{\delta,k}\hat{n}_ke^{i\vec{k}\cdot\vec{\delta}} - (J + 2N\mu_B\vec{B} + N\mu_e\vec{E})xS + N(\varphi - J)x^2S^2$$

$$+ (2JxS + 2\mu_B\vec{B} - \mu_e\vec{E} - 2S\varphi)\sum_k\hat{n}_k + (\varphi - J)\sum_k(\hat{n}_k)^2 \tag{3}$$

where $\hat{n}_k = \hat{a}_k^+\hat{a}_k$ is the number of magnons in state k and N is the total number of atoms in the system. Note that for one dimensional z number of neighbors, $\frac{1}{z}\sum_\delta e^{i\vec{k}\cdot\vec{\delta}} = 2\cos(ka)/z$, where a is the nearest neighbors distance.

Then, employing the limit to long wavelength excitation $(ka << 1)$ so that $\cos(ka) \approx 1 - k^2a^2/2$ and considering only the nearest neighbors (i.e., $z = 2$), Eq. (2) can be rewritten as

$$\hat{H} = \sum_k\hat{n}_k\omega_k + \{-(J + 2N\mu_B\vec{B} + N\mu_e\vec{E})xS + N(\varphi - J)x^2S^2 + (\varphi - J)\sum_k(\hat{n}_k)^2\}. \tag{4}$$

For non-interacting magnons, we can write $\hat{H} = \hat{H}_{mag} + E_0$ neglecting the last term involving magnon-magnon scattering; where

$$E_0 = -(J + 2N\mu_B B + N\mu_e E)xS + N(\varphi - J)x^2S^2 + (\varphi - J)\sum_k(\hat{n}_k)^2.$$

Hence,

$$\hat{H}_{mag} = \sum_k\hat{n}_k\omega_k, \tag{5}$$

where

$$\omega_k = JxSk^2a^2 + 2\mu_B B + \mu_e E - 2S\varphi, \tag{6}$$

is the overall magnon dispersion, whose variation with the applied fields and anisotropic energy is plotted and discussed in our previous work (Mesfin Birile *et al.,* 2020).

RESULTS AND DISCUSSION

The magnon specific heat capacity of the (Ga, Fe)Sb DMS

The expression for specific heat, C_{mag} of the diluted magnetic semiconductor system would be obtained from internal energy U of magnons given by (constant term E_0 does not contribute to magnon heat capacity and gives rise to energy gap in the magnon spectrum (Mesfin Birile *et al.,* 2020)).

$$U = \sum_k <\hat{n}_k> \omega_k, \tag{7}$$

where $\sum_k <\hat{n}_k>$ is the total number of magnons excited in all modes at temperature T and $<\hat{n}(k)> = (e^{\beta\omega_k} - 1)^{-1}$ is the number of spin waves with wave vector k in a single mode in

which $\beta = (k_B T)^{-1}$. Hence, substituting Eq.(6) into (7),

$$U = \sum_k \frac{Rk^2 + F}{e^{\beta(Rk^2+F)} - 1} = \frac{R}{(2\pi)^3} \int_0^\infty \frac{k^4}{ce^{vk^2} - 1} dk + \frac{F}{(2\pi)^3} \int_0^\infty \frac{k^2}{ce^{vk^2} - 1} dk , \qquad (8)$$

where $c = e^{\beta F}$, $v = \beta R$, $R = JxSa^2$, and $F = 2\mu_B B + \mu_e E - 2SD$. We have also introduced B, E, and D for the magnitudes of the MF, EF and MAE, respectively.

For v > 1 the Bose-Einstein (BE) function is given by

$$B_{v-1} = \frac{1}{\Gamma(v)} \int_0^\infty \frac{x^{v-1}}{\frac{1}{z}e^x - 1} dx. \qquad (9)$$

For small z ($z << 1$), classical limit $T >> 0$, we can use the expression

$$B_{v-1}(z) = \sum_{n=1}^\infty \frac{z^n}{n^v}. \qquad (10)$$

From Eq. (9) and Eq. (10), we get

$$\sum_{n=0}^\infty \frac{z^n}{n^v} \Gamma(v) = \int_0^\infty \frac{x^{v-1}}{\frac{1}{z}e^x - 1} dx. \qquad (11)$$

Using Eq. (11) into Eq. (8) with $v = 3/2$ and $z = 1/c = e^{-\beta F}$, results

$$U = \frac{R}{2(2\pi)^3 v^{5/2}} \int_0^\infty \frac{x^{(5/2-1)}}{\frac{1}{z}e^x - 1} dx + \frac{F}{2(2\pi)^3 v^{3/2}} \int_0^\infty \frac{x^{(3/2-1)}}{\frac{1}{z}e^x - 1} dx$$

$$= \frac{R}{2(2\pi)^3 v^{5/2}} \sum_{n=1}^\infty \frac{e^{(-\beta F)^n}}{n^{5/2}} \Gamma\left(\frac{5}{2}\right) + \frac{F}{2(2\pi)^3 v^{3/2}} \sum_{n=1}^\infty \frac{e^{(-\beta F)^n}}{n^{3/2}} \Gamma\left(\frac{3}{2}\right)$$

. $\qquad (12)$

Assuming that the first term ($n = 1$) is much larger than all other terms, Eq. (12) simplifies to

$$U \cong \frac{P}{x^{3/2}} \left(\frac{3}{2} k_B T^{5/2} e^{-F/(k_B T)} + FT^{3/2} e^{-F/(k_B T)} \right),$$

, $\qquad (13)$

where $P = \frac{1}{32\pi^{5/2}} \left(\frac{k_B}{JSa^2} \right)^{3/2}$. Following the last expression magnon specific heat, C_{mag}, could be obtained from the partial derivative of internal energy with respect to temperature, $C_{mag} = \partial U/\partial T$, hence

$$C_{mag} \cong \frac{P}{x^{3/2}} \left(\alpha T^{3/2} + \gamma FT^{1/2} + \xi \frac{F^2}{\sqrt{T}} \right) e^{-F/(k_B T)},$$

$\qquad (14)$

where α, γ and ξ are numerical constants.

For the purpose of analysis the following parameters are used; the structure of *(GaFe)Sb* is considered to be *fcc* as of the host material with lattice parameter *a = 6.09593 Å*. Scanning tunneling electron circular dichroism measurement reveal that the structure does not change with doping (Tu. *et al.,* 2016]. In *Fe³⁺* the *3d* electrons would give rise to S = 5/2, μ_B= 9.2741 x 10²⁴ J/T = 0.0579 *meV/T*, $\mu_e \approx$ 0.08625 *C.m,* and *J ≈ 0:0365 meV*.

The magnon specific heat of the material is explained with respect to impurity concentration, magnitudes of the MF, EF and MAE, as shown in Figs. 1-5.
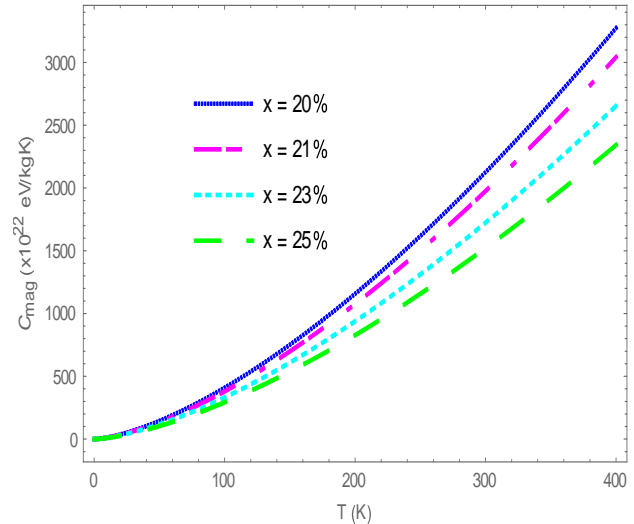
Figure 1. Magnon specific heat vs. temperature for different values of *x* when B = E = D = 0.

Figure 1 shows zero magnon specific heat at absolute zero and increase exponentially with temperature. The specific heat tends to dwindle as the magnetic impurity concentration x increases, *B*, *E*, and *D* being set to zero. This could lower the heating up and magnetic disordering in the material leading to enhanced carrier conductivity and long-range parallel orientation of *Fe³⁺ 3d* spins. In such cases Eq. (13) turns out to retrieve the typical characteristic T³/² law [Kŏnig et.al., 2000].
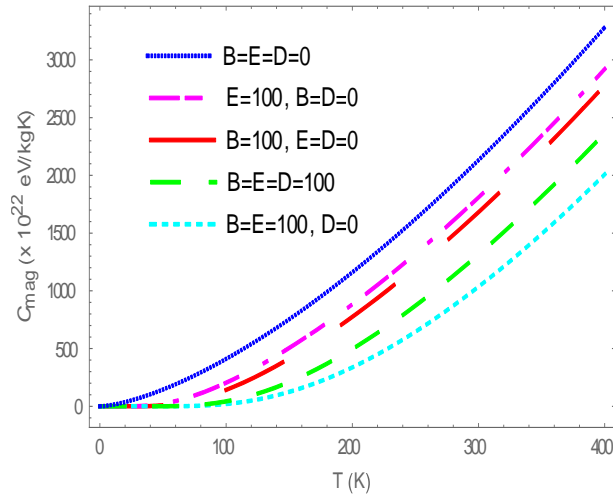
Figure 2. Magnon specific heat vs. temperature for the same values of *B*, *E*, and *D*, separately and all together, successively at *20% dopant concentration*.

Figure 2 illustrates the difference in the exponential increase of the magnon specific heat with only *B*, when *E* and *D* are set to zero; with only *E*, when *B* and *D* are set to zero; with only *D*, when *E* and *B* are set to zero; and with their combination as temperature increases. The specific heat increase is observed with temperature when both MF and EF are turned on compared to separate impinging, conversely to the contribution of the magnetic anisotropic energy.
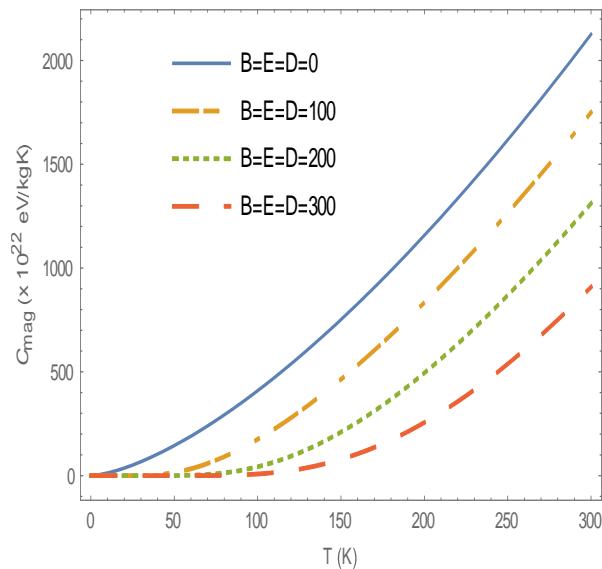
Figure 3. Magnon specific heat vs. temperature for varied similar values of *B*, *E* and *D* considered simultaneously at a concentration *x = 20%*.
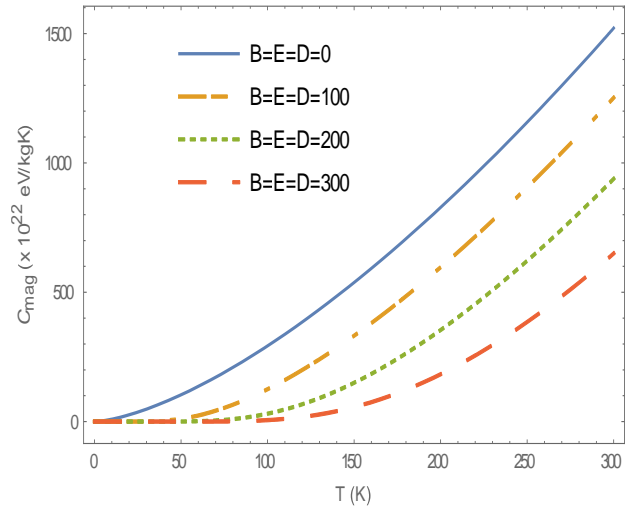
Figure 4. Magnon specific heat as a function of temperature with the same values of *B*; *E* and *D* simultaneously at a concentration of *x = 25%*.
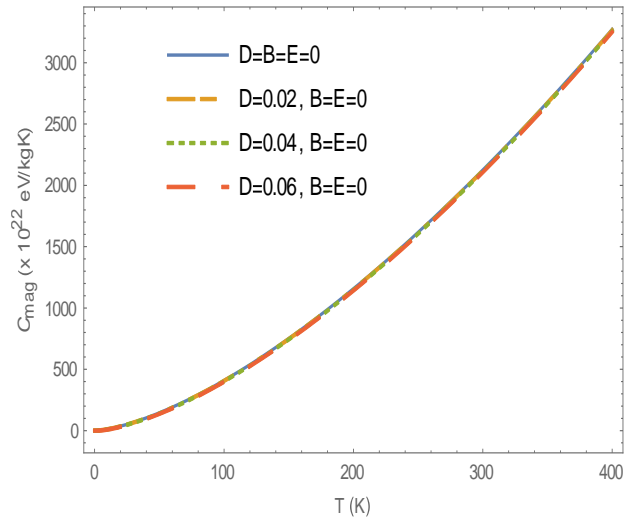
Figure 5. Magnon specific heat as a function of temperature for different values of *D* at the concentration *x = 20%* with *B* and *E* set to zero.

Figure 3 shows how the exponential raise in the specific heat decreases as temperature increases with the increase of *E*, *B*, and *D* simultaneously and uniformly at a concentration of *x = 20%*, and decrease further for further increase of impurity concentration as shown in Fig. 4. These could indicate the augmentation of magnon density in the *Fe/(GaSb)* DMS material in agreement with previous theoretical results for the case of *Ga₁₋ₓMnₓAs* (Chernet Amente *et al*., 2010) and *Zn₁₋ₓFeₓS* DMS (Twardowski *et al*., 1991).

However, the inclusion of magnetic anisotropic energy into the basic Hamiltonian has resulted in slight increase in magnon specific heat. This is illustrated in Fig. 5. The effect of the anisotropic energy is actually very small and very difficult to identify in the absence of EF and MF, perhaps both fields could enhance the anisotropic energy itself. The anisotropy is material dependent and some DMSs can be more anisotropic than the others. The value of *D* can be guided by specific material and applications.

Le and Yarmohammadi (Le *et al.*, 2019) have also studied magnon transport in Lieb lattice using Heisenberg model and including Dzyaloshinskii-Moriya interaction (Kim *et al.*, 2018) and obtain similar results, however, they have not included anisotropy. Le *et al.* (Le *et al.*, 2018; Le *et al.*, 2019) also investigated magnon impurity interaction effect on the magnon heat capacity on the Lieb lattice using similar model.

The magnetic susceptibility of the (Ga,Fe) Sb DMS

At a temperature *T* , the magnetization per site is given by

$$M(T) = M(0) - g\mu_B \sum_k \hat{n}_k , \qquad (15)$$

where *M(0)* is magnetization at absolute zero temperature and *g* = 2 for a system of spin ½ particles.

Since the system is attributed to resonate in bulk, Eq. (15), requires integration over a space as,

$$M(T) = M(0) - \frac{g\mu_B}{(2\pi)^3} \int_0^\infty \frac{k^2}{ck^{vk^2} - 1} dk , \qquad (16)$$

which can be simplified into

$$\frac{M(T)}{M(0)} = 1 - \frac{Y}{x^{3/2}} T^{3/2} e^{-F/(k_B T)} , \qquad (17)$$

where *Y* is a constant representing $g\mu_B(k_B)^{3/2}/[32\pi^{5/2}(JS)^{3/2}a^3]$.

The corresponding magnetic susceptibility of the system,

$$\chi = \frac{\partial M(T,B)}{\partial B} = \frac{Q}{x^{3/2}} T^{1/2} e^{-F/(k_B T)} , \qquad (18)$$

where *Q* is another constant given by $Y(2\mu_B/k_B)$.

The temperature gradient of Eq. (18) shows that the magnetic susceptibility is the area under the curves below the maximum picks which

corresponds to the Curie temperatures as illustrated in Figs. 6-9. As temperature increases, the curves increase until maximum $\nabla_T \chi$ is attained and then decrease exponentially with further increasing of temperature.

$$\nabla_T \chi = \frac{Q}{x^{3/2}} (T^{-1/2} + FT^{-3/2}) e^{-F/(k_B T)} . \qquad (19)$$

Figure 6 shows the temperature gradient of magnetic susceptibility vs. temperature for random choice of impurity concentrations, 20%, 21%, 23%, and 25% with *B* = *E* set to five and *D* set to zero. The area under the curve, for the temperature interval from 230 *K* to at which $\nabla_T \chi$ reaches its maximum, significantly reduce. This shows that the magnetic susceptibility is dropping and hence ferrimagnetic, antiferromagnetism and/or paramagnetism is overwhelming as the impurity spin concentration increases.
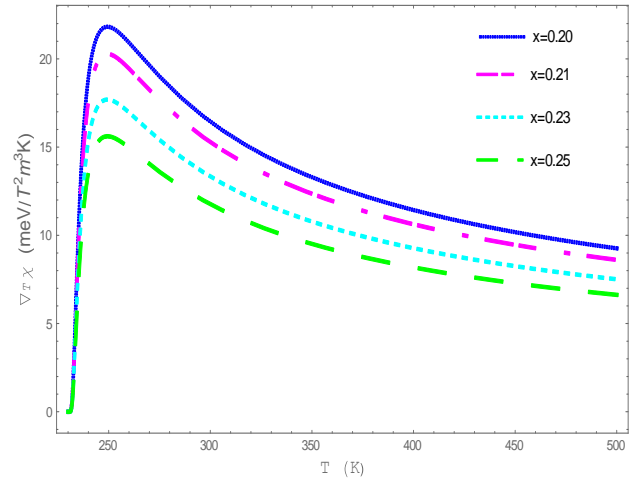
Figure 6. Temperature dependence of magnetic susceptibility for different values of *x*, *B* and *E* being set to five and *D* to zero.

Figure 7 compares the effects of *E, B*, and *D* when tuned on separately or simultaneously for the choice of 20% magnetic spin concentration. The illustrated four different cases indicate that maximum magnetic susceptibly is attained when electric and magnetic fields are tuned on and subjected to similar temperature variation. From the figure, inclusion of magnetic anisotropy energy leads to suppression of the susceptibility as it prevents alignment of magnetic spins.
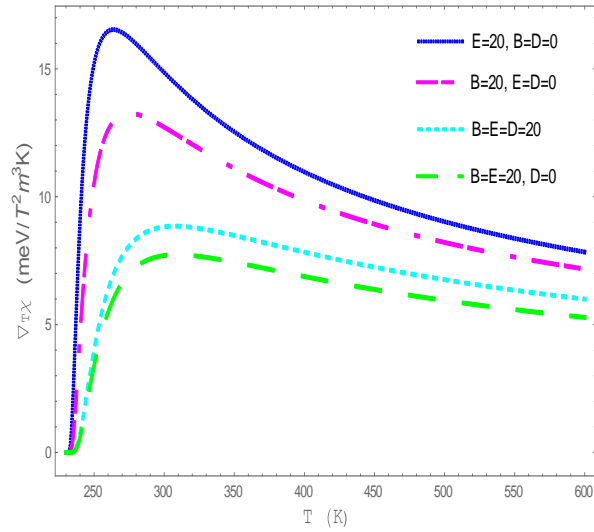
Figure 7. Temperature dependence of the magnetic susceptibility of *GaFeSb* for the same values of *E, B, D* and 20% magnetic impurity concentration.

Figure 8 also illustrate the enhancement of the magnetic susceptibility when the values of the combination of *B* and *E* increase at a concentration *x* = 20%, *D* being set to zero. On the other hand, the decrease in the peak of the temperature vs. $\nabla_T \chi$, in the absence of *E* and *B*, shown in Fig 9, envisage the reduction of the magnetic susceptibility as *D* increases.
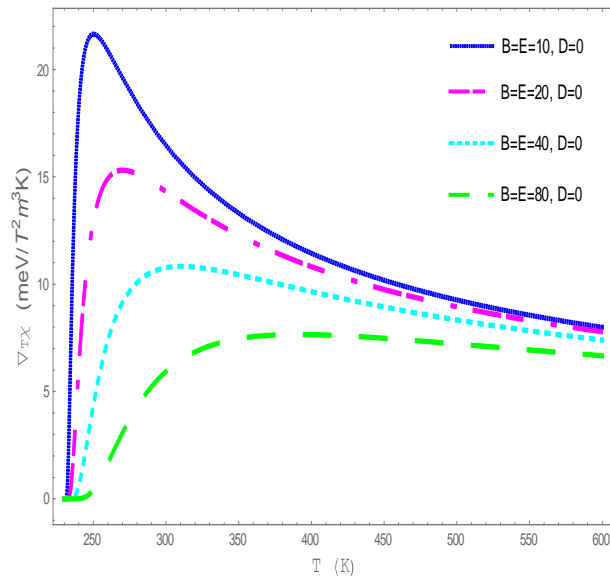
Figure 8. Temperature dependence of magnetic susceptibility with different values of *B = E* at a concentration of *x* = 20% and *D = 0*.
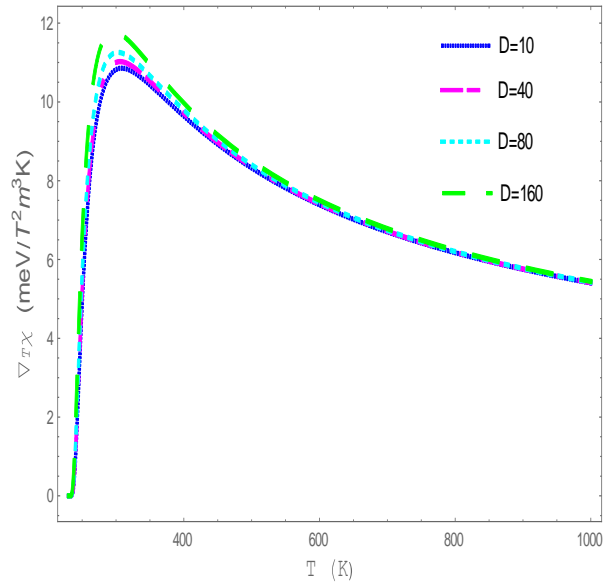
Figure 9. Temperature gradient of magnetic susceptibility vs. temperature for different values of *D* at *x* = 20%, and *E = B = 20*.

CONCLUSIONS

The magnon heat capacity C_{mag} and magnetic susceptibility χ of a ferromagnetic semiconductor $(Ga_{x-1}Fe_x)Sb$ have been theoretically studied. Their expressions have been obtained as functions of magnetic dopant concentration *x* using Heisenberg localized spin model in the presence of external electric field, magnetic field and magnetic anisotropy. C_{mag} and χ have been plotted for varies values of concentration *x* as functions of temperature *T*. The results demonstrate that it is possible to manipulate these magnetic properties of the diluted magnetic semiconductors by electric field, magnetic field and also magnetic anisotropy which are very important for spintronic device applications. The study is important as electric field controlled ferromagnetism is very much needed from the stand point of developments in the fast developing field of spintronics. The inclusion of magnetic anisotropy has also considerable practical significance in the design of magnetic materials for commercial importance. The results obtained are in broad agreement with recent experimental and theoretical findings.

REFERENCES

1. Boukari, H., Kossacki, P., Bertolini, M., Ferrand, D., Cibert, J., Tatarenko, S., Wasiela, A., Gaj, J.A., Dietl, T. (2002). Light and Electric Field Control of Ferromagnetism in Magnetic Quantum Structures. *Phys. Rev.* B **88**, 207204.

2. Bouzerar, G., Kudrnovsky, J., and Bruno, P. (2003). Disorder effects in diluted ferromagnetic semiconductors. *Phys. Rev. B* **68**, 205311.

3. Chernet Amente and Singh, P. (2010). Photo-excitation and spin wave scattering effects on specific heat of the (Ga_{1-x}, Mn_x) as diluted magnetic semiconductor. *Int. J. Phys. Sci.* **5**: 274.

4. Chernet Amente Geffe, (2018). Low temperature anomaly of light stimulated magnetization and heat capacity of the 1D diluted magnetic semiconductors. *AIP Advances* **8**: 035317.

5. Climente, J.I., Korkusinski, M., Hawrylak, P., Planelles, J. (2005). Voltage control of the magnetic properties of charged semiconductor quantum dots containing magnetic ions. *Phys. Rev. B* **71:** 125321.

6. Dietl, T., Ohno, H., Matsukura, F., Cibert, J., and Ferrand, D. (2000). Zener model description of ferromagnetism in zinc-blende magnetic semiconductors. *science* **287**: 1019.

7. Dietl, T. (2001). Why Ferromagnetic Semiconductors?, *Acta Phys. Pol. A,* **100**: 139.

8. Esmailian, A.H., Kanjouri, F., Mohammadi, N., Mahloojian, M.R., Abbasi, N. (2012). Spin-waves in Stoner ferromagnetic phase of a two-dimensional electron system. Solid State Phenomena **190**, 15.

9. Furdyna, J.K. (1988). Diluted magnetic semiconductors, J. Appl. Phys. **64**, R29.

10. Hilbert, S. and Nolting, W. (2005). Magnetism in (III,Mn)V diluted magnetic semiconductors: Effective Heisenberg model. *Phys. Rev. B* **71**: 113204.

11. Holstein, T. and Primakoff, H. (1940). Field Dependence of the Intrinsic Domain Magnetization of a Ferromagnet. *Phys. Rev,* **58:** 1098.

12. Jungwith, T., Jairo Sinova, Maṡek, J., Kucera, J., MacDonald, A.H. (2006). Theory of ferromagnetic (III, Mn) V semiconductors. *Rev. Mod. Phys.* **78**: 809.

13. Kane, M.H. (2007). Investigation of the Stability of Wide band gap Diluted Magnetic Semiconductor for Spintronics. Doctoral Thesis, Georgia Institute of Technology.

14. Kim, S., Ueda, K., Gyungchoon Go, Peong-Hwa Jang, Kyung-Jin Lee, Abderrezak Belabbes, Aurelien Manchon, Motohiro Suzuki, Yoshinori Kotani, Tetsuya Nakamura, Kohji Nakamura, Tomohiro Koyama, Daichi Chiba, Kihiro. Yamada, T., Duck-Ho Kim, Takahiro Moriyama, Kab-Jin Kim, and Teruo Ono, (2018). Correlation of the Dzyaloshinskii-Moriya interaction with Heisenberg exchange and orbital asphericity. *Nature Comm.* **9**: 1649.

15. Kõnig, J., Lin, H. and MacDonald, A.H. (2000). Theory of Diluted Magnetic Semiconductor Ferromagnetism. *Phys. Rev. Lett.* **84**: 5628.

16. Lashkarev, G.V., Sichkovskiyi, V.I., Radchenko, M.V., Karpina, V.A., Butorin, P.E., Dmitriev, O.I., Lazorenko, V.I., and Slynko, E.I. (2009). Diluted magnetic semiconductors based on II-VI, III-VI, and IV-VI compounds. *Low Temp. Phys.* **35**: 62.

17. Le, P.T.T., Hoi, B.D., and Yarmohammadi, M. (2018). Magnon-impurity interaction effect on the magnonic heat capacity of the Lieb lattice. AIP Advances **8**, 125317.

18. Le, P.T.T., and Yarmohammadi, M. (2019). Impurity-tuning of phase transition and midstate in 2D spin Lieb lattice. Physica E: Low-dimensional Systems and Nanostructures **474**, 137.

19. Le, P.T.T., and Yarmohammadi, M. (2019). Magnonic heat transport in the Lieb lattice, J. Magn. and Magn. Matt. **469**, 623.

20. Manyala, N., DiTusa, J.F., Aeppli, G., and Ramirez, A.P. (2008) Doping a semiconductor to create an unconventional metal. *Lett. Nature* **454**: 976.

21. Matthias, B.T., Bozorth, R.M., and Van Vleck, J.H. (1961). Ferromagnetic Interaction in EuO. *Phys. Rev. Lett.* **7:** 160.

22. Mauger, A., and Godart, C. (1986). The magnetic, optical, and transport properties of representatives of a class of magnetic semiconductors: The europium chalcogenides. *Phys. Rep.* **141**: 51.

23. Mesfin Birile Woldetsadik, Pooran Singh, and Chernet Amente Geffe, (2020). Effects of magnetic field, electric field, and magnetic anisotropic energy on the magnetic properties of Fe alloyed GaSb diluted magnetic semiconductor. *AIP Advances* **10**: 035120.

24. Munekata, H., Ohno, H., Von Molnar, S., Segmuller, A., Chang, L. L., and Esaki, L. (1989). Diluted magnetic III-V semiconductors. *Phys. Rev. Lett.* **63**: 1849.

25. Ohno, H., Chiba, D., Matsukura, F., Omiya, T., Abe, E., Dietl, T., Ohno, Y., Ohtani, K. (2000). Electric-Field control of ferromagnetism. *Nature* **408**: 21.

26. Ohno, H., Matsukura, F., and Ohno, Y. (2002). Semiconductor Spin Electronics. General Report, Cutting edge l.

27. Peaton, S. J., Abernathy, C.R., Norton, D.P., Hebard, A.F., Park, Y.D., Boatner, L.A., and Budai, J.D. (2003). Materials Science and Engineering, R. **40**, 137.

28. Sanvito, S., Hill, N.A. (2002). Prediction of enhanced ferromagnetism in (Ga, Mn) As by intrinsic defect manipulation. *J. Mag. Mag. Materials* **238**: 252.

29. Tu, N.T., Hai, P.N., Anh, L.D., and Tanaka, M. (2015). Magnetic properties and intrinsic ferromagnetism in (Ga,Fe)Sb ferromagnetic semiconductors. *Phys. Rev. B.***92**: 144403.

30. Tu, N.T., Hai, P.N., Anh, L.D., and Tanaka, M. (2016). High-temperature ferromagnetism in heavily Fe-doped ferromagnetic semiconductor (Ga,Fe)Sb. *Appl. Phys. Lett.* **108**: 192401.

31. Twardowski, A., Swagten, H.J.M., and de Jonge, W.J.M. (1990). Low-temperature specific heat of the diluted magnetic semiconductor Hg_{1-x-y},Cd_yFe_xSe. *Phys. Rev. B* **42**: 2455.

32. Twardowski, A., Swagten, H.J.M., and de Jonge, W.J.M., and Demianiuk, M. (1991). Magnetic properties of the diluted magnetic semiconductor $Zn_{1-x}Fe_xS$. *Phys. Rev. B* **44**: 2220.

33. Wolf, S.A., Awschalom, D.D., Buhrman, R.A., Daughton, J.M., Von Molnar, S., Roukes, M.L., Chtchelkanova, A.Y., and Treger, D.M. (2001). Spintronics: A spin-based electronics vision for the future. *Science* **294**: 1488.

34. Yosida, K. (1957). Magnetic Properties of Cu-Mn Alloys. *Phys. Rev.* **106**: 893.

35. Xiu, F., Wang, Y., Kim, J., Hong, A., Tang, J., Jacob, A.P., Zou, J., Wang, K.L. (2010). Electric-field controlled ferromagnetism in high-Curie-temperature $Mn_{0.05}Ge_{0.95}$ quantum dots. *Nat. Mater.* **9:** 337.

36. Zutic, I., Fabian, J., and Das Sarma, S. (2004). Spintronics: Fundamentals and applications, *Rev. Mod. Phys.* **76**: 323.